

## Supporting information for ‘**Functionalized chitosan adsorbents allow recovery of palladium and platinum from acidic aqueous solutions**’

### **SI1. Synthesis and characterization of metal chelating compounds**

SI1 A: Synthesis and characterization of 1,10-phenanthroline-2,9-dicarbaldehyde (PDC)

SI1 B: Synthesis and characterization of [2,2'-bipyridine]-5,5'-dicarbaldehyde (BPDC)

SI1 C: Synthesis and characterization of 8-hydroxyquinoline-2-carbaldehyde (HQC)

### **SI2. Detailed assignment of FTIR spectra from chitosan and its derivatives**

SI2 A: FTIR spectrum of chitosan

SI2 B: FTIR spectrum of Ch-PDC

SI2 C: FTIR spectrum of Ch-BPDC

SI2 D: FTIR spectrum of Ch-GA-HQC

### **SI3. Elemental analysis of chitosan and its derivatives**

### **SI4. BET specific surface area determination of chitosan and its derivatives**

### **SI5. Point of Zero Charge ( $\text{pH}_{\text{PZC}}$ ) determination**

### **SI6. Parameters of the pseudo-first-order kinetic model**

### **References**

## SI1. Synthesis and characterization of metal chelating compounds

### SI1 A: Synthesis and characterization of 1,10-phenanthroline-2,9-dicarbaldehyde (PDC)

2.1 equivalents of  $\text{SeO}_2$  (50.4 mmol, 5.59 g), 120 mL dioxane and 3.4 mL demineralized water were placed in a round bottom flask and heated to 120 °C. When the mixture started refluxing, 1 equivalent neocuproine (24.0 mmol, 5.00 g) was dissolved in 96.6 mL of dioxane and was added to the flask. This mixture was refluxed for 2 h. After reaction, the hot mixture was filtered. The retained black solids were washed with dioxane and chloroform. Finally, the combined solvents were evaporated *in vacuo*, resulting in 5.00 g 1,10-phenanthroline-2,9-dicarbaldehyde.<sup>1-3</sup> Yield = 88%, orange powder. **M. p.:** 230 °C; **FTIR**  $\nu_{\text{max}}/\text{cm}^{-1}$ : 2850 (CH ald.) and 1695 (C=O),  **$^1\text{H-NMR}$**  (400 MHz, DMSO- $d_6$ ):  $\delta$  = 8.30 (2H, s,  $\text{H}^{5,6}$ ), 8.33 (2H, d,  $J$  = 8.2 Hz,  $\text{H}^{3,8}$ ), 8.81 (2H, dd,  $J$  = 8.2 Hz,  $J$  = 0.7 Hz,  $\text{H}^{4,7}$ ), 10.36 (2H, d,  $J$  = 0.7 Hz, CHO).

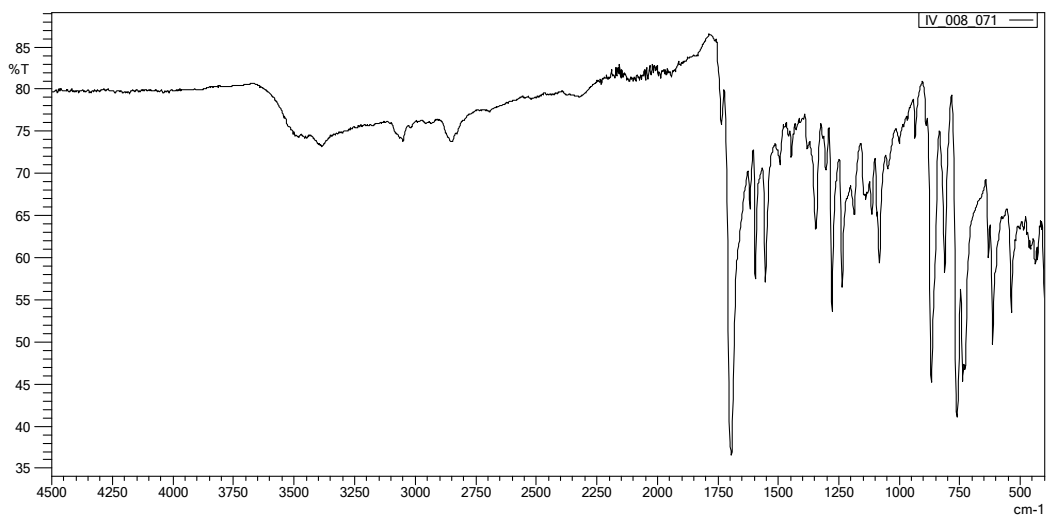


Fig. S11 FTIR spectrum of PDC

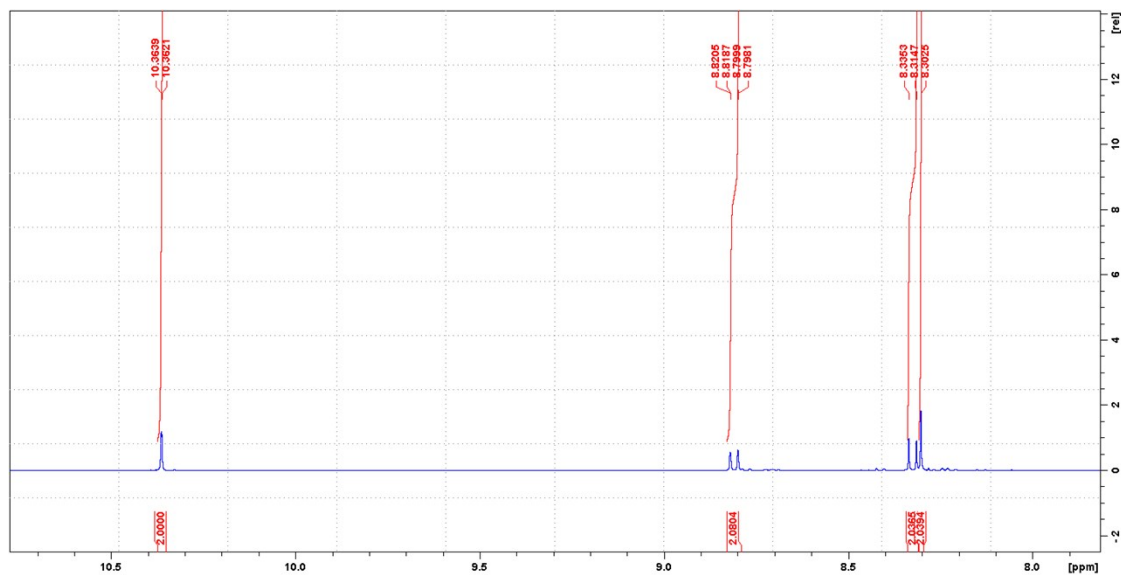


Fig. S12 Zoom of NMR spectrum of PDC

### S11 B: Synthesis and characterization of [2,2'-bipyridine]-5,5'-dicarbaldehyde (BPDC)

The synthesis of BPDC starts from 5,5'-bis(bromomethyl)-2,2'-bipyridine, which is derived from 5,5'-dimethyl-2,2'-bipyridine. To a solution of 1 equivalent of 5,5'-dimethyl-3,3'-bipyridine (27.1 mmol, 5.0 g) in 163 mL  $\text{CCl}_4$ , 2.2 equivalents *N*-bromosuccinimide (59.6 mmol, 10.6 g) were added. This mixture was stirred for 10 min at room temperature, after which 0.042 equivalents benzoyl peroxide (1.1 mmol, 275.7 mg) were added. This mixture was refluxed for 5 h under argon atmosphere. After reaction, the mixture was cooled to room temperature and poured into 200 mL of demineralized water. The mixture was extracted with  $\text{CHCl}_3$  (4 x 200 mL) and the combined organic fractions were washed with demineralized water (2 x 50 mL), dried with anhydrous  $\text{MgSO}_4$ , filtered and evaporated *in vacuo*. The product was recrystallized in methanol, and washed with cold methanol. 5.15 g of 5,5'-bis(bromomethyl)-2,2'-bipyridine (56%) was obtained. In a next step, a mixture of 5,5'-bis(bromomethyl)-2,2'-bipyridine (14.3 mmol, 4.88 g),  $\text{NaHCO}_3$  (239.3 mmol, 20.10 g) and 151 mL DMSO was heated to 115 °C. After 3.5 h, the mixture was cooled to room temperature and poured into 200 mL of demineralized water. The precipitated product was filtered and dissolved in 500 mL of  $\text{CH}_2\text{Cl}_2$ . This organic layer was washed with demineralized water (3 x 100 mL) and dried over anhydrous  $\text{MgSO}_4$ . After filtration, the solvent was evaporated *in vacuo*, resulting in 1.50 g [2,2'-bipyridine]-5,5'-dicarbaldehyde.<sup>4,5</sup> Yield = 49%. **M. p.**: 228 °C; **FTIR**  $\nu_{\text{max}}/\text{cm}^{-1}$ : 2812 and 2756 (CH ald.), 1678 (C=O); **<sup>1</sup>H-NMR** (400 MHz,  $\text{CDCl}_3$ ):  $\delta$  = 8.35 (2H, d,  $J$  = 8.1 Hz,  $\text{H}^{\text{ar}}$ ), 8.72 (2H, d,  $J$  = 8.1,  $\text{H}^{\text{ar}}$ ), 9.17 (2H, s,  $\text{H}^{6,6'}$ ), 10.21 (2H, s, CHO).

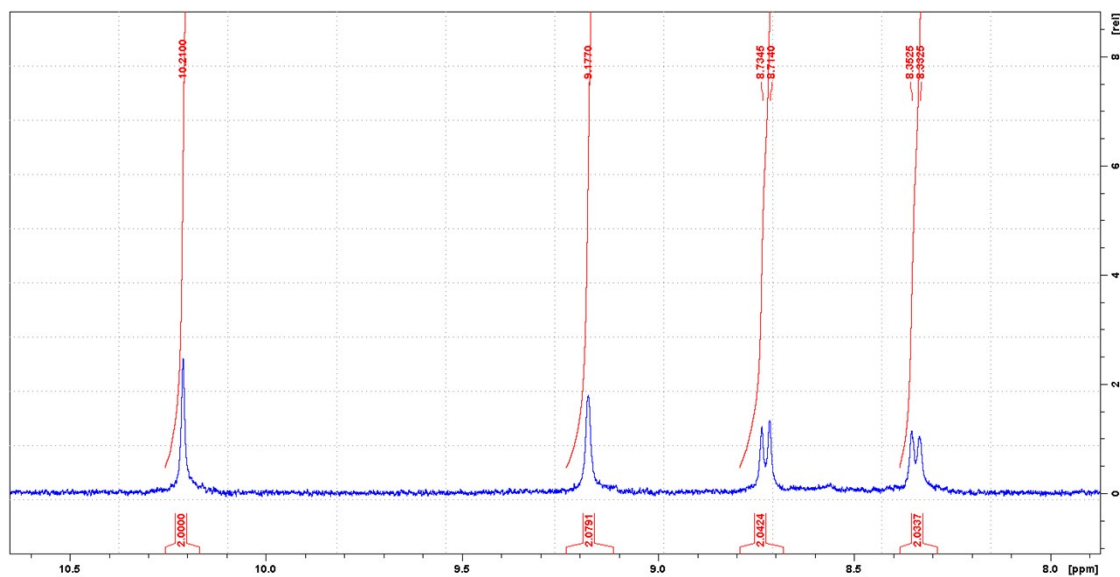
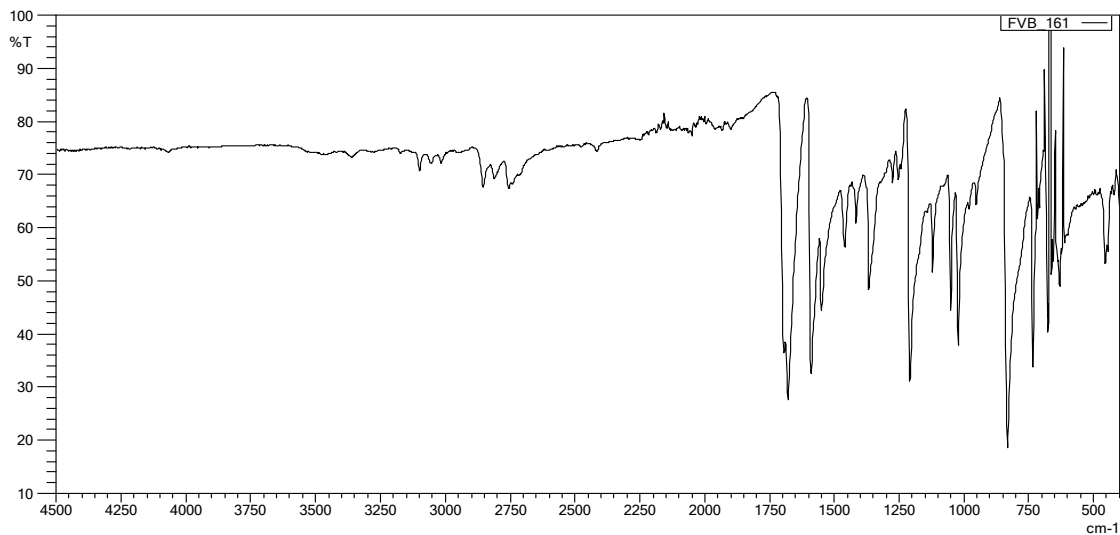


Fig. S13 FTIR spectrum of BPDC

Fig. S14 Zoom of NMR spectrum of BPDC

### S11 C: Synthesis and characterization of 8-hydroxyquinoline-2-carbaldehyde (HQC)

A mixture of 1 equivalent 2-methylquinolin-8-ol (6.28 mmol, 1.00 g), 1.24 equivalents  $\text{SeO}_2$  (7.79 mmol, 0.86 g), 8 mL demineralized water and 80 mL EtOAc was refluxed. After 48 h, the mixture was cooled to room temperature, filtered over a celite bed, rinsed and the solvents were evaporated *in vacuo*. After purification by column chromatography ( $\text{SiO}_2$ , petroleum ether:ethyl acetate, 95:5), 0.50 g 8-hydroxyquinoline-2-carbaldehyde was obtained. Yield = 46%. **M. p.**: 95 °C; **FTIR**  $\nu_{\text{max}}/\text{cm}^{-1}$ : 2835 (CH ald.), 1703 (C=O);  **$^1\text{H-NMR}$**  (400 MHz,  $\text{CDCl}_3$ ):  $\delta$  = 7.28 (1H, dd,  $J$  = 7.7 Hz,  $J$  = 0.9 Hz,  $\text{H}^5$ ), 7.43 (1H, dd,  $J$  = 8.2 Hz,  $J$  = 0.9 Hz,  $\text{H}^5$ ), 7.62 (1H, t,  $J$  = 8.0 Hz,  $\text{H}^6$ ), 8.06 (1H, d,  $J$  = 8.5 Hz,  $\text{H}^3$ ), 8.14 (1H, s, OH), 8.32 (1H, dd,  $J$  = 8.4 Hz,  $\text{H}^4$ ), 10.22 (1H, s, CHO).

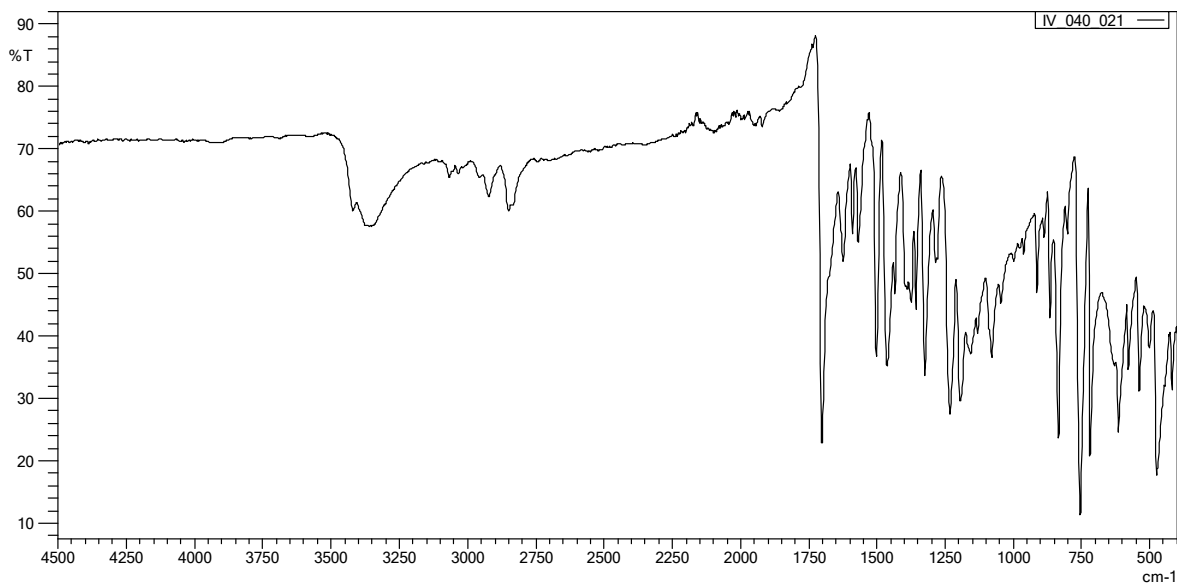


Fig. S15 FTIR spectrum of HQC

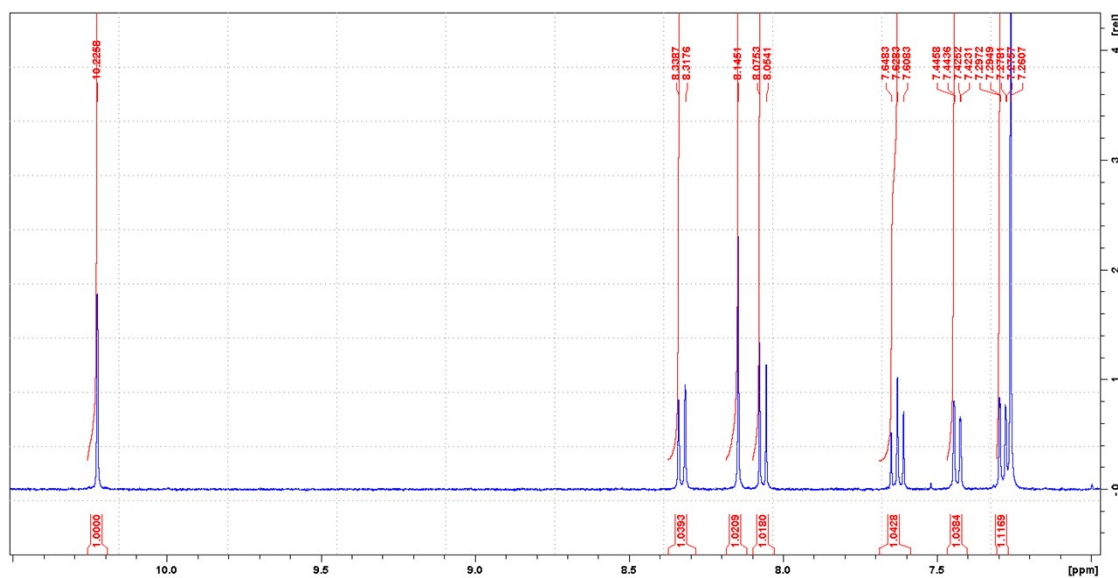


Fig. S16 Zoom of NMR spectrum of HQC

## S12 Detailed assignment of FTIR spectra from chitosan and its derivatives

### S12 A: FTIR spectrum of chitosan

Characteristic bands of the chitosan were visible at  $3288\text{ cm}^{-1}$  and  $3354\text{ cm}^{-1}$  (Fig. S17). The two peaks for chitosan indicate N-H stretching of primary amines and O-H stretching. The bands at  $2870\text{ cm}^{-1}$  and  $1377\text{ cm}^{-1}$  are due to C-H symmetric stretch and C-H bending vibration, respectively. The bands at  $1649\text{ cm}^{-1}$ ,  $1572\text{ cm}^{-1}$  and  $1309\text{ cm}^{-1}$  are attributed to the amide I (C=O), amide II (N-H) and amide III (C-N) bonds, respectively. The band around  $1024\text{ cm}^{-1}$  is attributed to the combined effects of C-N stretching vibration of primary amines and the C-O stretching vibration from the primary alcohol in chitosan. The band at  $893$  is attributed to the glucosidic C-O-C stretching.<sup>6</sup>

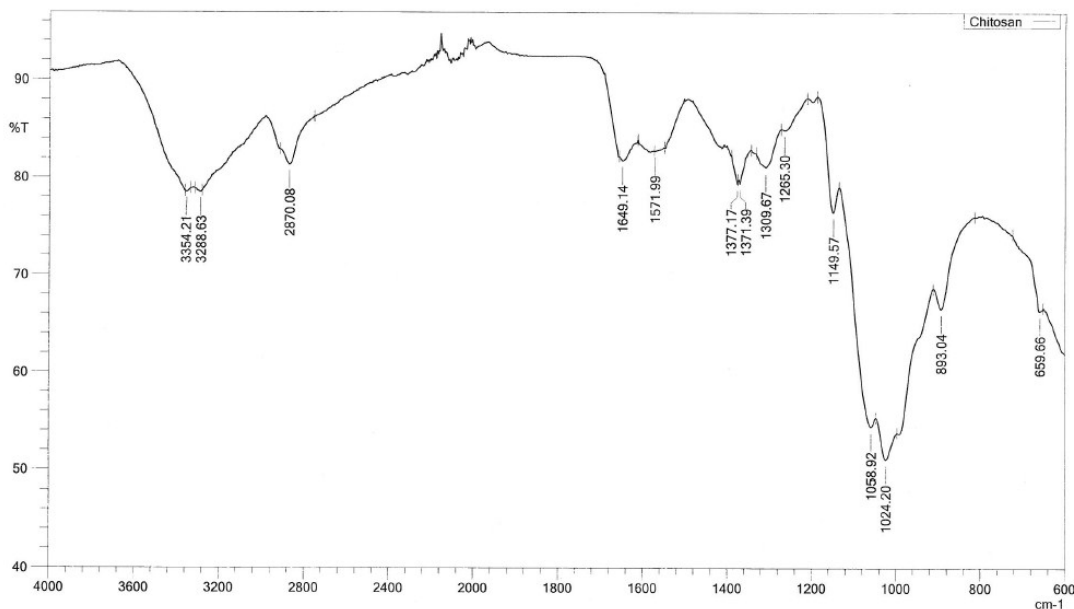


Fig. S17 FTIR spectrum of chitosan

### S12 B: FTIR spectrum of Ch-PDC

The broad band at  $3305\text{ cm}^{-1}$  shows the overlapping of O-H and N-H stretching vibration, together with N-H secondary amine stretching of the cross-linked chitosan (Fig. S18). The bands at  $2872\text{ cm}^{-1}$  and  $1371\text{ cm}^{-1}$  are due to C-H symmetric stretch and C-H bending vibration, respectively. The bands at  $1641\text{ cm}^{-1}$  and  $1548\text{ cm}^{-1}$  and  $1305\text{ cm}^{-1}$  are attributed to the amide I, II a, III bonds, respectively. The bands around  $1026\text{ cm}^{-1}$  is attributed to the combined effects of C-N stretching vibration of primary amines and the C-O stretching vibration from the primary alcohol in chitosan.<sup>6</sup> The band at  $893$  is attributed to the glucosidic C-O-C stretching. The band around  $856\text{ cm}^{-1}$  indicates the presence of aromaticity, which are coming from the 1,10-phenantroline ring system.

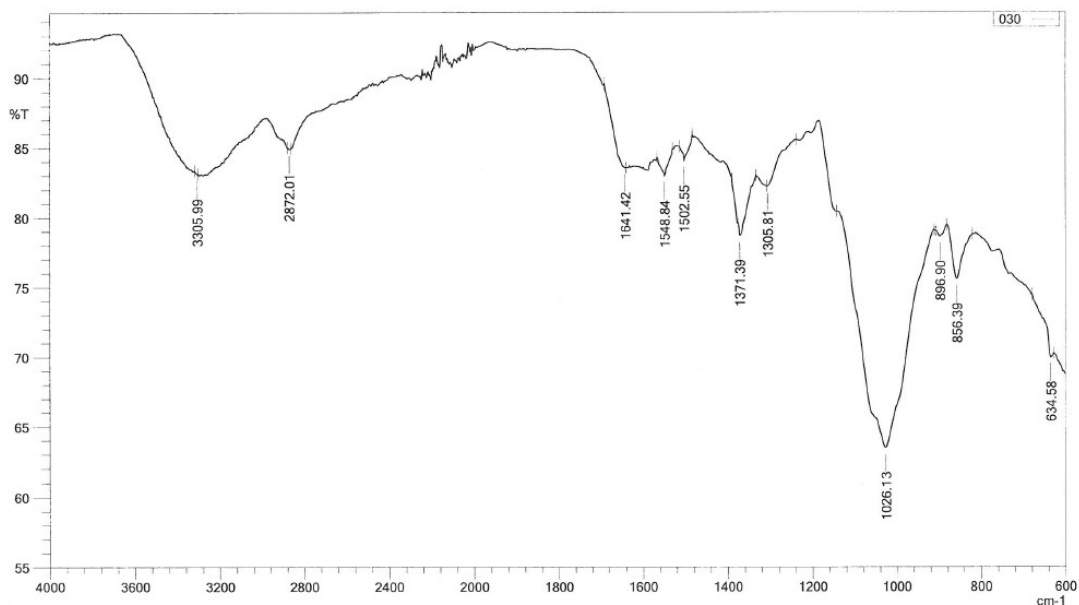


Fig. S18 FTIR spectrum of Ch-PDC

**S12 C: FTIR spectrum of Ch-BPDC**

The broad band at 3298 cm<sup>-1</sup> shows the overlapping of O-H and N-H stretching vibration, together with N-H secondary amine stretching of the cross-linked chitosan (Fig. S19). The bands at 2868 cm<sup>-1</sup> and 1371 cm<sup>-1</sup> are due to C-H stretching and C-H bending vibration, respectively. The peaks at 1649 cm<sup>-1</sup>, 1566 cm<sup>-1</sup> and 1309 cm<sup>-1</sup> are attributed to the amide I, II and III bands, respectively. The bands around 1024 cm<sup>-1</sup> and 1055 cm<sup>-1</sup> are attributed to the combined effects of C-N stretching vibration of amines and the C-O stretching vibration from the primary alcohol in chitosan.<sup>6</sup> The peak at 1244 cm<sup>-1</sup> indicates the presence of a nitrogen atom in an aromatic system. The peak at 835 cm<sup>-1</sup>, 752 cm<sup>-1</sup> and 717 cm<sup>-1</sup> indicate the presence of aromaticity, resulting from the pyridine rings.

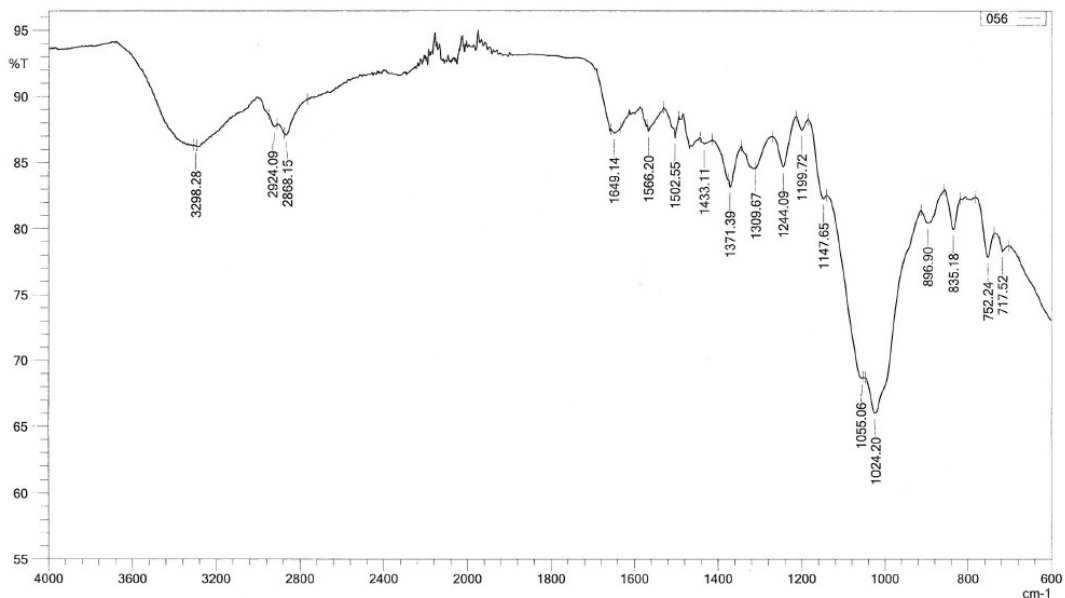


Fig. S19 FTIR spectrum of Ch-BPDC

#### SI2 D: FTIR spectrum of Ch-GA-HQC

The broad band at  $3300\text{ cm}^{-1}$  shows the overlapping of O-H or N-H stretching vibration, together with N-H secondary amine stretching of the cross-linked chitosan (Fig. SI10). The bands at  $2883\text{ cm}^{-1}$  and  $1381\text{ cm}^{-1}$  are due to C-H symmetric stretching and C-H bending vibration, respectively. The bands at  $1649\text{ cm}^{-1}$  and  $1548\text{ cm}^{-1}$  are attributed to the amide I and II bands, respectively. The bands around  $1022\text{ cm}^{-1}$  and  $1066\text{ cm}^{-1}$  are attributed to the combined effects of C-N stretching vibration of amines and the C-O stretching vibration from the primary alcohol in chitosan.<sup>6</sup> Band around  $2981\text{ cm}^{-1}$  and  $1381\text{ cm}^{-1}$  is due to C-H vibration, coming from the  $\text{CH}_2$  cross-linking carbons. The peaks around  $742\text{ cm}^{-1}$  and  $819\text{ cm}^{-1}$  indicate the presence of aromaticity due to quinolone grafting onto chitosan.

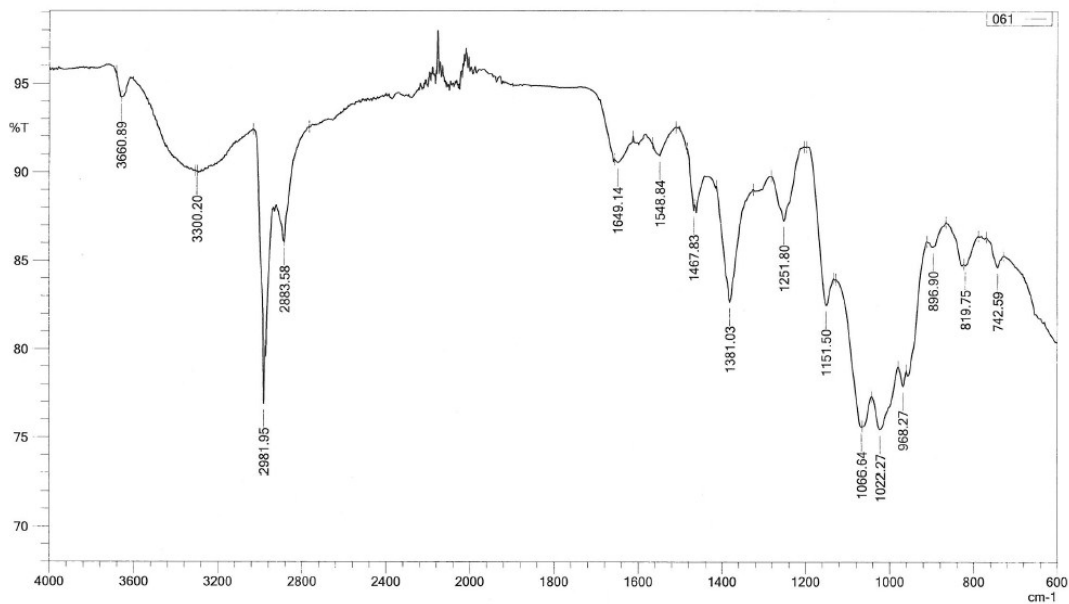


Fig. SI10 FTIR spectrum of Ch-GA-HQC

### SI3. Elemental analysis of chitosan and its derivatives

**Table SI1** Elemental analysis of chitosan and its derivatives

Compound	Nitrogen (%)	Carbon (%)	Hydrogen (%)	Total (%)	N/C (%)
Ch	7.229	41.600	7.316	56.145	17.4
Ch-PDC	8.520	49.092	5.299	62.911	17.4
Ch-BPDC	8.910	52.138	6.598	67.646	17.1
Ch-GA-HQC	7.087	52.011	5.568	64.666	13.6

Elemental analysis shows that cross-linking of chitosan with PDC and BPDC has a minor influence on the nitrogen to carbon ratio (N/C) of these derivatives, compared to native chitosan (Table SI1). The derivatization with GA-HQC results in a lower N/C ratio. This difference can be attributed to the specific cross-linking and metal adsorbing compounds added to chitosan. In the case of Ch-GA-HQC, two carbon rich compounds were added, with only one nitrogen atom present in HQC. For the derivatization of Ch-PDC and Ch-BPDC only one compound (PDC or BPDC) was used that contains two nitrogen atoms.



#### SI4. BET specific surface area determination of chitosan and its derivatives

**Table SI2** Brunauer–Emmett–Teller (BET) surface areas of chitosan and its derivatives

Compound	SA <sub>BET</sub> (m <sup>2</sup> /g)
Ch	1
Ch-PDC	2
Ch-GA-HQC	1

An overview of the Brunauer-Emmett-Teller (BET) surface areas of chitosan and its derivatives is given in Table SI2. The surface area of Ch-BPDC was not determined. It is expected to be in the same range of the given surface areas (1-2 m<sup>2</sup>/g).

### SI5. Point of Zero Charge ( $\text{pH}_{\text{PZC}}$ ) determination

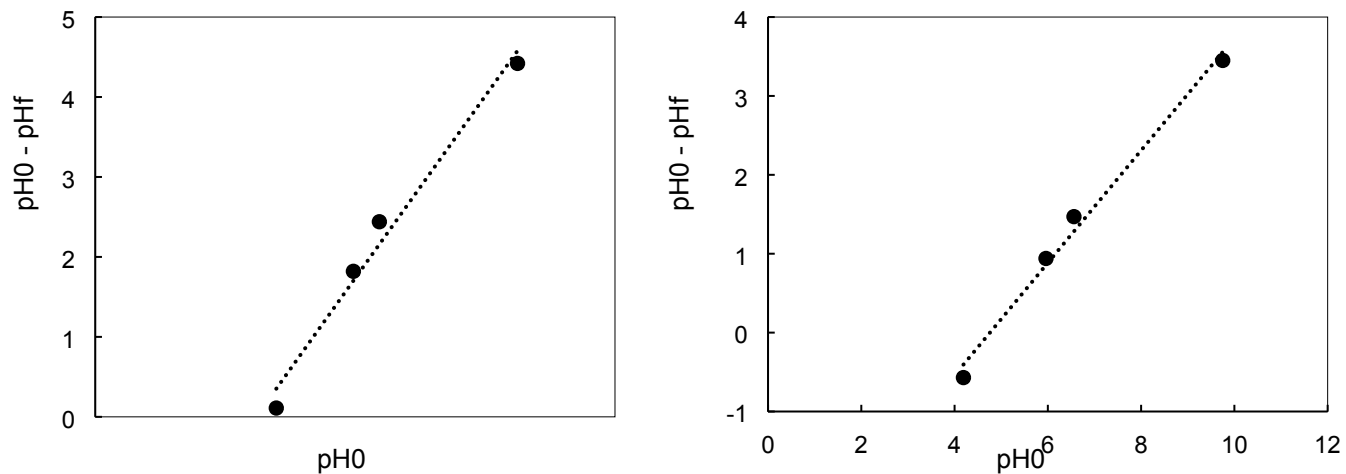


Fig. SI11 Difference in pH as a function of original pH of Ch-PDC (left) and Ch-GA-HQC (right)

The intersection of the line with the X-axis yields the  $\text{pH}_{\text{PZC}} = 3.72$  for Ch-PDC and  $\text{pH}_{\text{PZC}} = 4.76$  for Ch-GA-HQC (Fig. SI11). The  $\text{pH}_{\text{PZC}}$  of Ch-BPDC was not determined. Since the type of modification of the later compound closely resembles that of the other compounds, it is assumed that the  $\text{pH}_{\text{PZC}}$  of Ch-BPDC is in the same order (3.7 – 4.7). Adsorption characteristics were determined at pH 3 which is below the  $\text{pH}_{\text{PZC}}$  of all materials.

## S16. Parameters of the pseudo-first-order kinetic model

**Table S13** Parameters of the pseudo-first-order kinetic model for Pd and Pt adsorption on Ch-PDC, Ch-BPDC and Ch-GA-HQC with standard error (SE)

Element	Parameter	Ch-PDC (SE)	Ch-BPDC (SE)	Ch-GA-HQC (SE)
Pd	$q_{e,exp}$ (mg/g)	24.2 (0.1)	25.2 (0.1)	22.8 (0.1)
	$q_{e,cal}$ (mg/g)	23.9 (0.2)	25.1 (0.4)	21.8 (0.2)
	$k_1$ (min <sup>-1</sup> )	0.25 (0.01)	0.25 (0.03)	0.22 (0.01)
	R <sup>2</sup>	0.9965	0.9985	0.9782
Pt	$q_{e,exp}$ (mg/g)	25.0 (0.4)	24.8 (0.3)	24.8 (0.3)
	$q_{e,cal}$ (mg/g)	24.2 (0.8)	23.9 (0.6)	24.6 (0.2)
	$k_1$ (min <sup>-1</sup> )	0.18 (0.05)	0.26 (0.05)	0.12 (0.01)
	R <sup>2</sup>	0.9121	0.9537	0.9973

## References

- 1 N. T. Coogan, M. A. Chimes, J. Raftery, P. Mocilac and M. A. Denecke, *J. Org. Chem.*, 2015, **80**, 8684–8693.
- 2 J. C. García-Ramos, Y. Toledano-Magaña, L. G. Talavera-Contreras, M. Flores-Álamo, V. Ramírez-Delgado, E. Morales-León, L. Ortiz-Frade, A. G. Gutiérrez, A. Vázquez-Aguirre, C. Mejía, J. C. Carrero, J. P. Laclette, R. Moreno-Esparza and L. Ruiz-Azuara, *Dalt. Trans.*, 2012, **41**, 10164.
- 3 A. De Cian, E. DeLemos, J.-L. Mergny, M.-P. Teulade-Fichou and D. Monchaud, *J. Am. Chem. Soc.*, 2007, **129**, 1856–1857.
- 4 T. Yu, D. P.-K. Tsang, V. K.-M. Au, W. H. Lam, M.-Y. Chan and V. W.-W. Yam, *Chem. - A Eur. J.*, 2013, **19**, 13418–13427.
- 5 A. Helms, D. Heiler and G. McLendon, *J. Am. Chem. Soc.*, 1992, **114**, 6227–6238.
- 6 J. Kumirska, M. Czerwicka, Z. Kaczyński, A. Bychowska, K. Brzozowski, J. Thöming and P. Stepnowski, *Mar. Drugs*, 2010, **8**, 1567–1636.